Sustainable Structures
ISSN: 2789-3111 (Print); ISSN: 2789-312X (Online)
http://www.sustain-dpl.com/journal/sust
DOI: 10.54113/j.sust.2026.000096

ORIGINAL ARTICLE

Post-tensioning of structural members using natural fiber ropes

Ali Alraie[a], Saverio Spadea[b,*], Vasant Matsagar[c]

[a] Department of Civil, Environmental, Building Engineering and Chemistry, Polytechnic University of Bari, Via Edoardo Orabona, 4, 70126 Bari BA, Italy
[b] Department of Civil, Environmental, Building Engineering and Chemistry, Polytechnic University of Bari, Via Edoardo Orabona, 4, 70126 Bari BA, Italy
[c] Department of Civil Engineering, Indian Institute of Technology (IIT) Delhi, Hauz Khas, Delhi - 110 016, India
[*]Corresponding Author: Saverio Spadea. Email: saverio.spadea@poliba.it

Abstract: Natural fiber composites have recently gained popularity in construction due to their numerous benefits. Their applications include incorporation into the concrete mixture, potential replacement of steel reinforcement in reinforced concrete components, and strengthening of structural elements. Notably, despite their relatively low stiffness, these materials exhibit a good load-bearing capacity in tension, indicating that post-tensioning may represent the most effective technique for employing these materials in conjunction with concrete. Surprisingly, this technology has yet to be considered in structural concrete research. The current study presents a thorough analytical, experimental, and numerical approach to assess the efficacy of post-tensioning concrete members using natural jute fiber (NJF) ropes. Preliminary analytical investigations reveal that the proposed post-tensioning can improve a beam's flexural strength by 5.9% when a single rope is used. The experimental validation supports the reliability of the analytical findings, with numerical analysis indicating a potential improvement of 16.3% when the number of ropes used on the same beam is increased to four. Overall, the enhanced flexural performance of concrete structural elements through post-tensioning with NJF ropes appears promising. This novel technique not only improves the flexural performance of concrete members but also has the potential to address critical issues related to conventional post-tensioning, such as the corrosion of steel cables. Additionally, it offers increased flexibility by facilitating the replacement of ropes when required, making it a practical and versatile solution for several concrete applications in the construction industry.

Keywords: natural jute fiber, NJF, post-tensioning rope, concrete beam, flexural capacity, serviceability

1 Introduction

Fibers have been employed to strengthen bricks and pottery since the dawn of civilization. These fibers can be categorized as either synthetic or natural fibers. While synthetic fibers are manufactured from chemical compounds, natural fibers are made from natural materials from plants, animals, or minerals. Plant-based natural fibers include those sourced from cotton, linen, hemp, jute, etc. In contrast, animal-sourced natural fibers comprise silk, wool, and hair. Additionally, there exists a third category of natural fibers, including mineral, non-metallic, and inorganic fibers, such as asbestos and basalt fibers.

Received: 11 March 2025; Received in revised form: 14 July 2025; Accepted: 29 August 2025

Natural fibers are renewable raw materials that are readily available worldwide. Their production requires minimal industrialization, which typically results in lower manufacturing costs. They possess good thermal, acoustic, and electrical insulation properties. The waste generated from these fibers can be thermally valorized, allowing for energy generation subsequent to the product's lifespan [1]. Latest developments in the field of composite science, along with the emergence of natural fibers, offer substantial opportunities to introduce renewable materials that can positively impact global sustainability [2–4]. From an environmental standpoint, the sustainability index for the natural kenaf and jute fibers is the highest, thanks to their carbon use efficiency [5]. However, despite their advantages, natural fibers also have disadvantages, including low stiffness, variable tensile strength, significant moisture absorption, limited durability, and susceptibility to fire. Additionally, proposing these fibers into the construction industry presents challenges due to insufficient knowledge and notable irregularities in their physical and mechanical characteristics, which arise from various factors, including soil, weather, and environmental conditions. Consequently, it is essential to consider these aspects while establishing design standards for structures reinforced with natural fibers [6,7].

The durability of natural fibers has been a persistent concern [8]. From a structural perspective, Ramakrishna et al. [9] observed a significant degradation in salient chemical components (cellulose and lignin) after 30 cycles of wetting and drying for 60 days. In terms of strength, certain fibers, such as coir and sisal, retained over half of the original tensile strength subsequent to submerging in water, whereas others, including jute and Hibiscus cannabinus, completely lost their tensile strength [9]. Furthermore, humidity was found to significantly accelerate creep strain in sandwich panels reinforced with natural fibers [10]. The creep strains in vegetable fiber concrete were noted 25% higher than those in plain concrete for jute and coir, and about 12% higher for bamboo fiber concrete at 60 days [11]. Amongst efforts to enhance the durability of natural fibers, hydrothermal and alkali treatments could significantly contribute to the durability and dimensional stability of the natural fiber ropes used as internal reinforcements in concrete structures [12]. It was reported that concrete slabs reinforced with coir ropes, when coated with epoxy resin, remained unaffected by acidic or sulfate environments over a two-year period, indicating good durability for the coir rope reinforced bio-composite concrete panels [8].

Natural fibers have been used in construction since the late 1970s. Short fibers from jute, coconut, bamboo, and coir were tested for cementitious and polymer concrete use. It was noted that incorporating these natural fibers improved ductility and durability while reducing shrinkage compared to plain concrete without any serious adverse effects [13–16]. The potential of rice husk for partially replacing cement in concrete mixtures was investigated. It was observed that this integration reduced the cost of concrete by 15% and decreased CO_2 emissions by 20%, in addition to mitigating the environmental pollution caused by burning rice residues [17,18]. Concerning mechanical properties, the inclusion of the short fibers of jute, sisal, rice straw, and palm leaf sheath in concrete did improve the tensile and compressive strengths of the cementitious composites [19–21]. In contrast, the incorporation of hemp fiber was associated with increased flexural strength while simultaneously decreasing the compressive strength and elevating the concrete's permeability [22]. Recently, it was reported that incorporating sisal fibers into the concrete mix not only enhanced its mechanical properties but also prolonged the setting time by utilizing the retained water, contributing to the hydration process [23]. Alternatively, natural fiber ropes were explored for use as internal reinforcement for structural concrete members [24]. The observation indicated that the deformation capacity could be improved by substituting as much as 50% of the steel reinforcement while maintaining 75% of the control beam's load capacity and serviceability factors.

The application of natural fibers extends to the external strengthening of structural elements. Experimental findings indicated that the external confinement of concrete cylinders with hybrid textile-reinforced mortar wraps, incorporating basalt and jute fibers, enhanced the load-bearing capacity by 51.9% [25]. Investigations on structural elements revealed that concrete beams strengthened with composite plates made from jute ropes demonstrated a 58% increase in flexural strength compared to control beams [26]. In another study, Huang et al. [27] noted that composite plates made from natural flax fabric-reinforced polymer could effectively strengthen and retrofit damaged or poorly designed RC beams, especially those affected by earthquakes. The cost-efficacy of FRP-confined concrete was also assessed, with jute fiber-reinforced polymer being the most economically efficient [28]. The utilization of natural fibers has also been expanded to include columns, where studies demonstrated that these materials could significantly enhance the structural performance of shear-critical reinforced concrete columns, achieving levels comparable to those established by CFRP sheets [29]. Additionally, natural fiber composites have been proposed for strengthening masonry walls, which has considerably improved the out-of-plane flexural and deformation capacities [30,31]. Alternatively, another approach has involved mortars reinforced with natural textile/fabric as external layers for strengthening masonry structures [32,33].

Numerous prior studies have primarily focused on incorporating short natural fibers in concrete. Only a few investigations have explored using natural fiber ropes as reinforcing and/or strengthening agents. Notably, research on using natural fiber ropes for post-tensioning applications on structural concrete beams is lacking. One main limitation of employing natural fiber ropes for reinforcing concrete structures is their low modulus of elasticity compared to traditional reinforcing materials. It is crucial to use reinforcing materials with a considerably higher stiffness than the cementitious matrix in reinforced concrete. This is necessary to effectively transfer tensile stresses from the concrete to the reinforcement and control cracking and deflection under serviceability limit states. In light of this, it was demonstrated that natural fiber ropes could effectively be utilized to enhance the flexural properties of non-primary structural elements made from foamed concrete, which has limited mechanical properties [34].

Despite their low tensile strength, natural fiber ropes can bear significant loads when an adequate quantity of fiber is used. However, the inherent flexibility of braided products often results in considerable deformation compared to conventional reinforcing materials. It is crucial to understand that the fundamental principle of concrete post-tensioning is based more on the compressive force exerted on the concrete than on the stiffness of the reinforcing material. Thus, the primary objective of the current study is to demonstrate the efficiency of using natural fiber ropes for post-tensioning in reinforced concrete. The concept was first introduced and assessed through a numerical investigation supported by experimental testing [35]. A comprehensive study is currently being carried out to further demonstrate the efficiency of the present technique through an in-depth analytical investigation and finite element analysis, aided appropriately with experimental validation. Given that conventional post-tensioned beams with steel cables are susceptible to corrosion, the current research proposes using NJF ropes as a substitute for post-tensioned steel cables while ensuring the protection of the concrete's steel tension reinforcement. Additionally, the finite element analysis explores the possibility of replacing the reinforcing steel with non-corroding fiber-reinforced polymer rebars, facilitating a steel-free concrete member. This design aims to enhance corrosion resistance. Overall, using natural fibers offers a sustainable, eco-friendly alternative to steel, potentially contributing to construction sustainability.

2 Natural Jute Fiber (NJF) Ropes

Jute is a low-price bast fiber that ranks second to cotton in production and usage [36]. Its fibers are derived from several plant components, including lignin, cellulose, pectin, and hemicellulose. Notably, jute fiber is entirely biodegradable, making it an environmentally sustainable option. It possesses considerable tensile strength while maintaining minimal extensibility, which is why it is predominantly employed in packaging agricultural products. Furthermore, jute is among the most versatile natural fibers, finding applications as raw materials in both the construction and farming industries.

A preliminary tensile test was necessary to assess the jute rope's mechanical properties. Multiple methods were followed to execute the test. The rope was initially gripped in the testing machine system, which led to premature failure of the gripped portion as a result of stress localization from the gripping effect. Subsequently, the rope was secured using tying ropes wrapped around the universal testing machine's upper and lower sections. However, this method caused the knots and tying ropes to loosen, resulting in significant sample deformation. Consequently, the actual deflection exceeded the maximum limit of travel of the machine without breaking the rope. After all, the rope was secured using steel tube anchors placed around the gripped zone, tied off with a knot. The machine's jaws have gripped the anchors while the jute rope was passed through them. This method proved successful, leading to the proper failure of the rope. Examples of natural fiber products available in the market and the tensile test on jute rope samples, 600 mm-long, are illustrated in **Fig. 1**. The experimentally obtained stress-strain response of the jute ropes, presented previously [35], is described here in **Fig. 2** for the sake of completeness of data for further investigation. The jute rope has exhibited an average tensile strength of 55.4 MPa, with an elastic modulus of 754.3 MPa. The notably low elastic modulus can be attributed to the braided structure of the rope, which causes the fiber yarns to straighten out. This results in considerable relaxation during the actual deformation of the yarns.

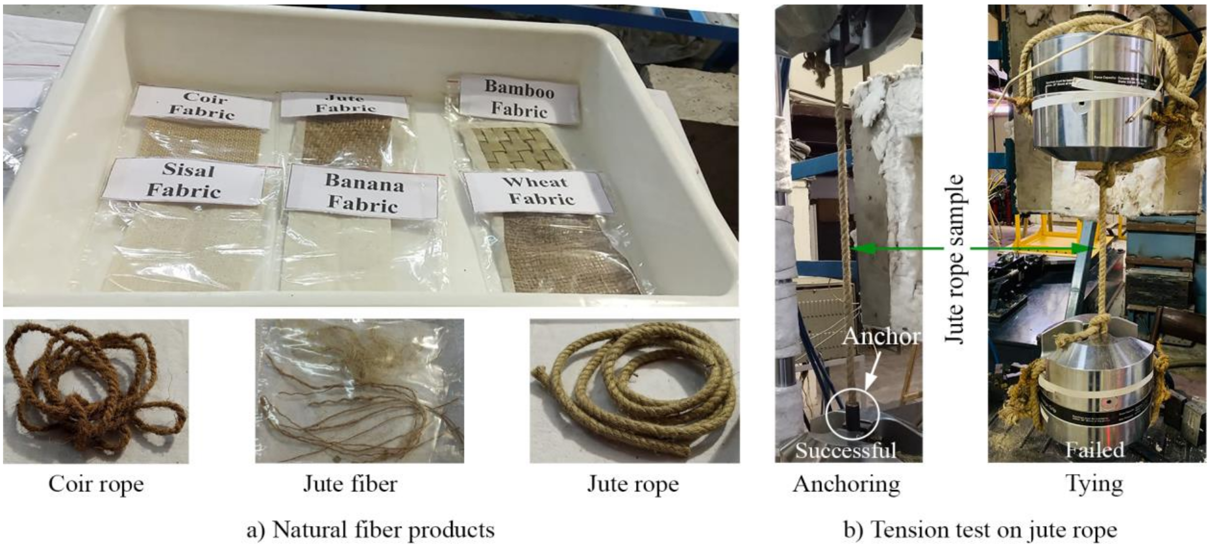

Fig. 1. a) Examples of natural fiber products; b) Tensile tests conducted on the jute ropes used in this study.

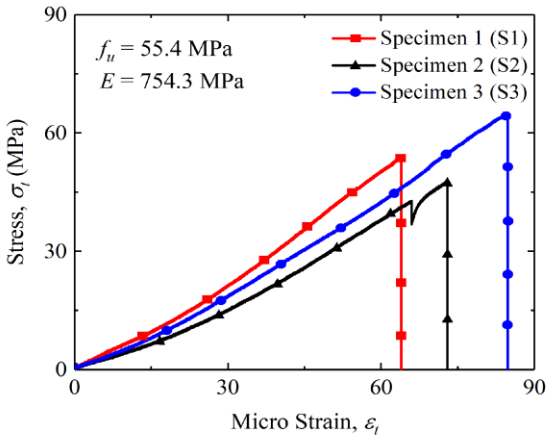

Fig. 2. Axial stress-strain response of the jute ropes, obtained experimentally.

3 NJF Post-tensioned RC Members

The NJF rope, previously characterized, was employed for post-tensioning structural members. An analytical investigation was carried out to estimate the structural behavior of such post-tensioned beams and investigate the proposed technique's efficiency. This was followed by an experimental campaign to validate the analytical findings. Subsequently, the finite element analysis assessed the proposed technique's efficacy with varying structural materials.

3.1 Analytical Prediction

Analytical investigations have been conducted to predict the behavior of the considered beams tested here, estimating the ultimate flexural capacity and comparing it with the experimental findings. Because of the relatively modest tensile strength of the rope and to maintain the benefit of such post-tensioning, it is required to check for the limit state of the NJF to ensure that the jute rope does not rupture before the tension steel does. The premature failure of the jute rope results in the loss of the benefit of post-tensioning; hence, it must not rupture before the steel reinforcement does, which is the reason for checking the balanced conditions corresponding to both materials separately. The cross-section of the beam with balanced conditions corresponding to the reinforcement materials is presented in **Fig. 3**. The balanced ratio corresponding to the steel reinforcements (ρ_{bs}) is given as [37]:

$$\rho_{bs} = 0.85\beta_1 \frac{f_c'}{f_{sy}} \frac{\varepsilon_{cu}}{\varepsilon_{cu} + \varepsilon_{sy}} \tag{1}$$

where f_c' is the concrete's compressive strength (MPa); f_{sy} is the steel's yield strength (MPa); ε_{cu} is the maximum compressive strain in concrete (0.003), and ε_{sy} is the strain in the steel reinforcement at yielding. The factor β_1 is the stress-block factor of concrete given by [38]

$$\beta_1 = 0.85 - \frac{0.05(f_c' - 27.5)}{6.9} \geq 0.65\,. \tag{2}$$

The balanced condition for a fragile reinforcing material, like jute, has a different meaning from that of steel. While this balanced condition signifies a simultaneous failure of both the concrete and the reinforcing material, it regards the yielding of steel as a failure indicator, a property absent in the brittle jute. Therefore, the balanced reinforcement ratio corresponding to the NJF post-tensioning rope (ρ_{bj}) can be expressed using Eq. (1), substituting the steel's yield characteristics with the ultimate properties of the NJF rope. This indicates that the balanced condition is reached when the concrete fails in compression at a strain ε_{cu} and the NJF rope ruptures at a strain ε_{ju} concurrently, conforming to the strain compatibility within the cross-section. These strains, in conjunction with the ratio of the concrete's compressive strength to the tensile strength of the NJF, establish the balanced ratio as

$$\rho_{bj} = 0.85\beta_1 \frac{f_c'}{f_{ju}} \frac{\varepsilon_{cu}}{\varepsilon_{cu} + \varepsilon_{ju}} \tag{3}$$

where f_{ju} and ε_{ju} are the tensile strength (MPa) and strain at failure of the NJF, respectively.

The reinforcement ratio is determined from the total area of the steel reinforcements. The contribution of the NJF rope area in the steel's limit state condition is determined based on the ratio of the actual tensile stress in the NJF at balance to the maximum tensile stress of steel. Similarly, the contribution of the steel reinforcement area in the jute's limit state condition is determined based on the ratio of actual tensile stresses in the steel at balance to the maximum tensile stress in the NJF. The actual reinforcement ratio is given as [39]

$$\rho = \frac{\sum_{i=1}^{p} A_{fi}\alpha_i}{bd_m} \tag{4}$$

where A_{fi} is the cross-section area of a reinforcement layer; α_i is the ratio of tensile stress of reinforcements in layer i at balance to the maximum tensile stress of steel; b is the beam width; d_m is the effective depth of the bottommost layer; and p is the total number of reinforcing layers.

The neutral axis depth is determined based on the equilibrium of compressive force in the concrete and tensile force in the reinforcement. In over-reinforced sections, the concrete reaches its ultimate compressive strain of 0.003 before steel yielding; hence, the strain in the reinforcements at failure will be less than ε_{sy}. The strain in the steel reinforcement (ε_s) and NJF post-tensioning rope (ε_j) at compressive failure is calculated as

$$\varepsilon_s = 0.003(d_s - c)/c \tag{5a}$$

$$\varepsilon_j = \varepsilon_{ji} + \Omega_u \frac{0.003(d_j - c)}{c} \tag{5b}$$

where d_s is the effective depth of the steel reinforcement; d_j is the NJF rope's effective depth; ε_{ji} is the initial post-tensioning stress in the NJF rope; c is the depth of neutral axis; and Ω_u is the ultimate bond reduction coefficient expressed as $5.4/(L_u/d_j)$ for two-point loading [39]. Here L_u is the distance between the ends of the post-tensioning rope.

In under-reinforced sections, the tensile stress in the reinforcements reaches the yielding point before concrete crushing; thereby, the resultant tensile forces are determined from the steel's yielding strain, i.e., the tensile strain in the unbonded NJF rope is calculated as

$$\varepsilon_j = \varepsilon_{ji} + \Omega_u \frac{\varepsilon_{sy}(d_j - c)}{(d_s - c)}. \tag{6}$$

Solving the horizontal equilibrium equation determines the depth of the neutral axis, and then the moment of resistance is obtained by solving the rotation equilibrium equation.

The geometrical and design details of the beam analyzed in this study are shown in **Fig. 3**. The beam has the following dimensions: 150 mm in width, 200 mm in depth, and 2000 mm in length. The clear span employed in flexural testing is 1800 mm. The concrete has a 35.5 MPa compressive strength. All beams have two 12 mm-diameter steel rebars as bottom reinforcement. Additionally, the post-tensioned beams are equipped with supplementary jute rope that has a diameter of 14 mm. The steel rebars are made from Grade 60 material, featuring a 411.4 MPa yield strength and a tensile strength of 622.7 MPa, while the jute's mechanical properties are stated earlier. Shear reinforcements consist of 6 mm-diameter steel rebars spaced at 120 mm. The beam is post-tensioned by 80% of the jute's tensile strength. A flexural analysis was conducted for both cases to evaluate the change in flexural capacity with post-tensioning: the beam with post-tensioning and the beam without it. The flexural capacities were obtained as 50.5 kN for the control beam and 53.4 kN for the jute-post-tensioned beam, indicating a 5.9% increase as a result of the NJF post-tensioning. The improved flexural capacity can be justified by the fact that post-tensioning induces initial tensile stresses in the upper concrete fibers while generating compressive stresses in the lower cross-section, surrounding the tension reinforcements. The pre-existing compressive stresses, which are transferred to the reinforcements, contribute to a supplementary strength balance by nullifying a portion of the tensile stresses induced by the applied loads. Consequently, this allows the reinforcement to withstand additional loads prior to yielding, leading to a higher load-carrying capacity. The analytical data, procedures, and findings leading to the above results are summarized and presented in **Tables 1a–1d**. The current analysis was further expanded by employing four NJF ropes instead of one, resulting in a flexural capacity of 62.1 kN, corresponding to a 23.0% improvement over the control beam.

3.2 Experimental Validation

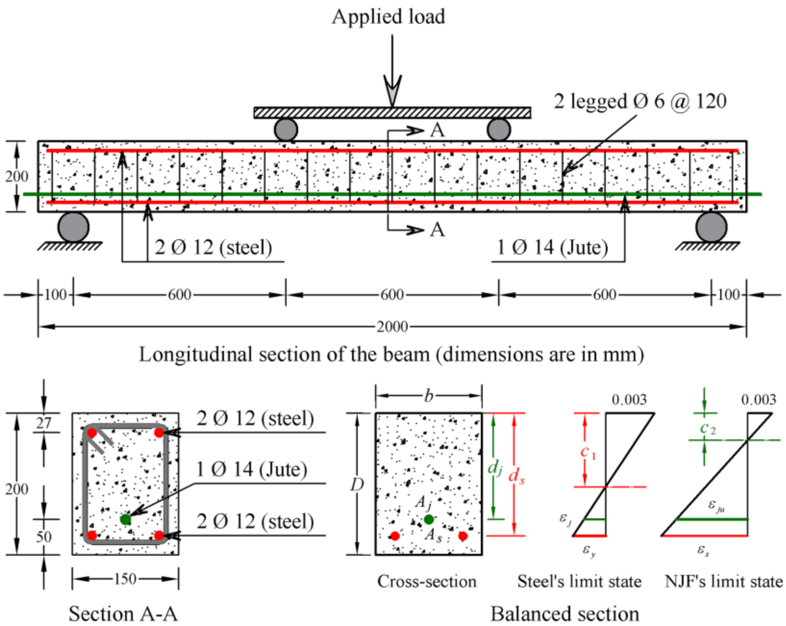

Fig. 3. Longitudinal and cross-sections of the considered beam with balanced conditions corresponding to the reinforcement materials.

The experimental campaign concerned the flexural performance of steel-reinforced concrete beams post-tensioned with a single jute rope, 14 mm in diameter. During casting, the beams were designed with internal ducts to house the NJF ropes. After hardening, a jute rope was passed through each beam, secured with anchors at the dead end, and tensioned at the opposite (live) end using a hydraulic actuator, without any grouting, thus keeping the rope unbonded. To improve the grip and prevent slippage at the anchor zone, the compressible rope was wrapped in cotton fabric. The post-tensioning setup included anchors, a hydraulic actuator, a load cell to measure the post-tensioning load, and a hollow steel casing that surrounded the rope and rested against the beam's end. A post-tensioning force of 6.8 kN was applied, corresponding to 80% of the jute rope's tensile strength. The laboratory post-tensioning setup is illustrated in **Fig. 4**.

Table 1a. Geometries and material properties of the analyzed beam

b (mm)	D (mm)	L (mm)	f_c' (MPa)	ε_{cu}	f_{sy} (MPa)	f_{su} (MPa)	d_s (mm)	E_s (MPa)	ε_{sy}	ε_{su}	A_s (mm^2)
150	200	1800	35.5	0.003	411.4	622.7	173	210000	0.00196	0.078	226.2

b, D, and L represent the width, overall depth, and span, respectively; f_c' and ε_{cu} are the characteristic compressive strength and maximum compressive strain in concrete, respectively; and f_{sy}, f_{su}, d_s, E_s, ε_{sy}, ε_{su}, and A_s are the yield strength, ultimate tensile strength, effective depth, elastic modulus, yield strain, ultimate tensile strain, and reinforcement area of the steel rebars, respectively.

Table 1b. Analytical findings of the reinforced (control) beam

β_1	ρ_{bs}	ρ	Design category	c (mm)	T_s (N)	C_c (N)	M_u (N·mm)	P_u (kN)
0.79	0.035	0.0087	Under-reinforced	25.95	93057	93057	15142184.7	50.47

β_1, ρ_{bs}, and ρ are the stress-block factor for concrete, balanced reinforcement ratio, and actual reinforcement ratio, respectively; c, T_s, and C_c are the neutral axis depth, tensile force in steel rebars, and compressive force in the concrete, respectively; M_u and P_u are the moment of resistance and flexural capacity, respectively.

Table 1c. Additional material properties and geometries of the jute-post-tensioned beam

f_{ju} (MPa)	d_j (mm)	E_j (MPa)	ε_{ju}	A_j (mm^2)	L_u (mm)
55.4	150	754.3	0.074	153.9	2000

f_{ju}, d_j, E_j, ε_{ju}, and A_j are the tensile strength, effective depth, elastic modulus, ultimate tensile strain, and area of the jute rope, respectively; and L_u is the distance between the ends of the post-tensioning rope.

Table 1d. Analytical findings of the beam post-tensioned with jute ropes

Ω_u	c (mm)	ε_{sy}	ε_{ji}	ε_j	T_s (N)	T_j (N)	C_c (N)	M_u (N·mm)	P_u (kN)
0.405	27.88	0.00196	0.0588	0.0594	93057	6900	99957	16030074	53.43

Ω_u is the ultimate bond reduction coefficient; ε_{ji}, ε_j, and T_j are the initial strain, actual strain, and tensile force in the jute rope, respectively; M_u and P_u are the moment of resistance and flexural capacity, respectively; and remaining terms are defined previously.

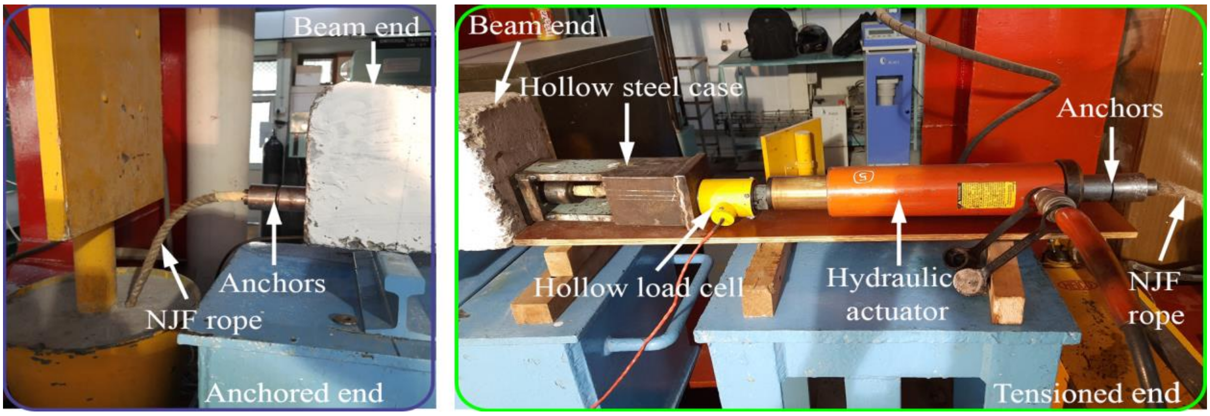

Fig. 4. Laboratory setup for post-tensioning on beams using jute ropes.

Following the post-tensioning application, the bending test was carried out until the beam failed. The bending test was performed on three identical samples for both the post-tensioned and control beams. **Fig. 5** illustrates the bending test with an elevational view of a tested beam. The beams have exhibited a tension-controlled failure, yielding the steel reinforcement, as evidenced by the significant deflection experienced by the beams. Thanks to strain compatibility, the jute rope's notably low stiffness (high stretchability) was crucial in preventing its rupture. **Fig. 6** compares the averaged load–deflection behaviors of both the control and post-tensioned beams loaded in incremental cycles. This loading method aims to facilitate a more comprehensive assessment of ductility, a topic not addressed in the current study.

It is evident from **Fig. 6** that the post-tensioned beam yielded 4.3% higher flexural capacity than the control beam. The difference between the flexural capacity measured here and that obtained from the analytical approach is justifiable. In the flexural analysis of the under-reinforced section, the moment of resistance is calculated considering the yield strength of the steel (411.4 MPa) conforming to the standard elastic-ideally plastic constitutive law. The yield strength here is significantly lower than the ultimate tensile strength of 622.7 MPa. This contributes to flexural strength, following an elastoplastic constitutive law in which strain hardening increases flexural capacity. Additionally, the concrete's compressive force is calculated analytically using a rectangular stress block approximation. Overall, the experimental validation demonstrated the proposed methodology and provided an informative indication of the improved flexural strength, which aligns with the analytical findings, and will be further evaluated through numerical simulation. It is to be noted that while this increase in flexural capacity is modest, it does exist and was accomplished using just a single jute rope due to limitations in laboratory equipment. This suggests that the structural strength could be further enhanced by increasing the number of post-tensioning ropes, which will be explored subsequently.

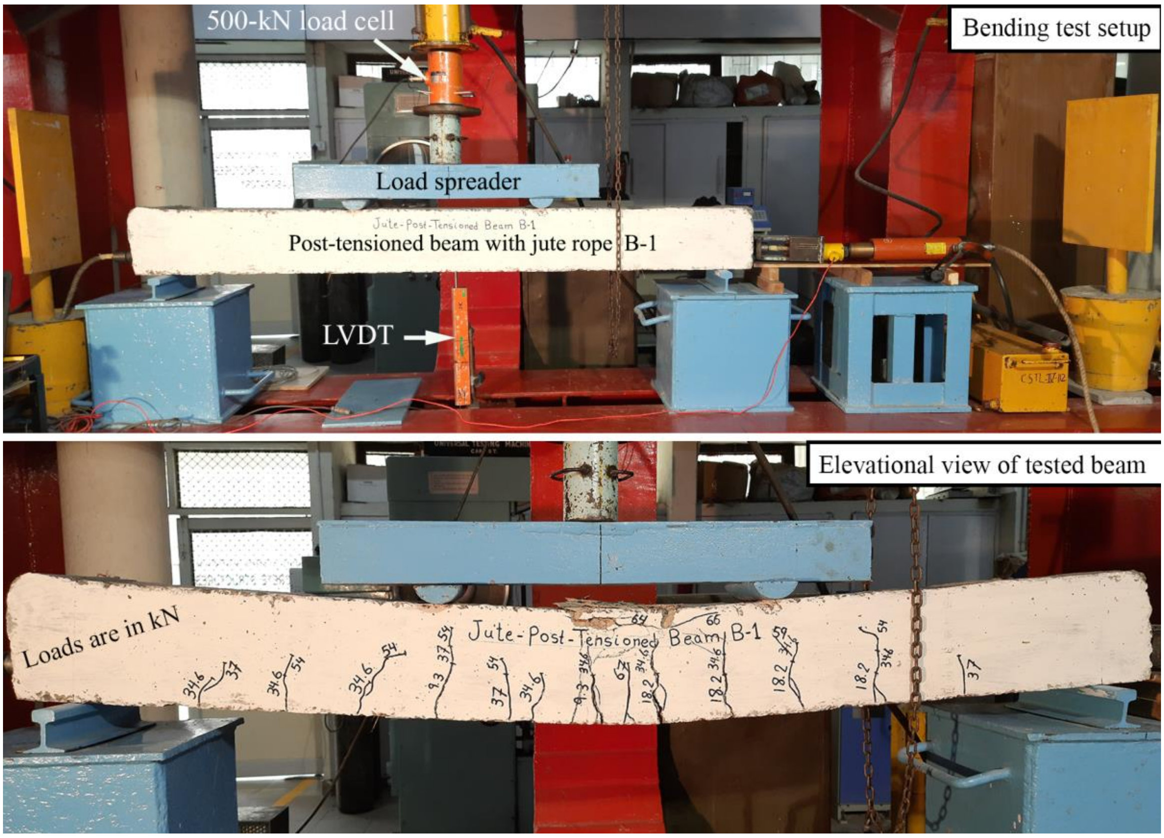

Fig. 5. Bending test on the jute-post-tensioned beam.

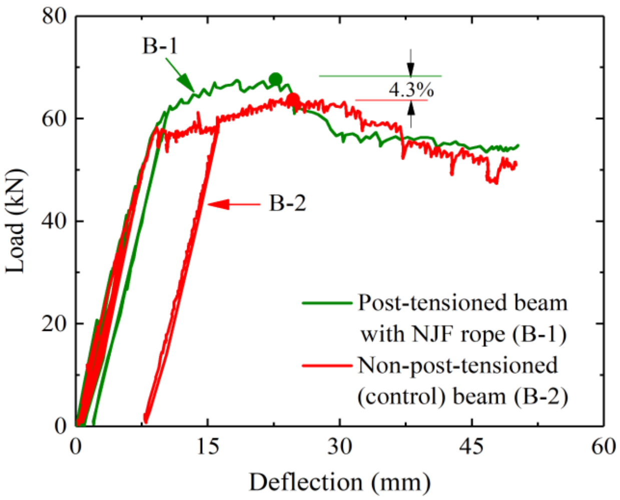

Fig. 6. Load–deflection curves of the control and post-tensioned beams tested in bending.

3.3 Numerical Analysis

For enhanced reliability, the beams' finite element analyses (FEA) were performed in ABAQUS®. An 8-node C3D8R elements were employed for modeling concrete [40,41], while 2-node three-dimensional elements (T3D2) were employed for modeling the steel [41]. A six-node linear triangular prism element (C3D6) was used to represent the whole geometry of the jute rope, which featured six degrees of freedom. The mechanical characteristics of the jute and steel are mentioned earlier. The concrete-reinforcement interaction was applied through the embedded region constraint [40,41], while the unbonded jute rope was anchored at the ends. An 80% existing tensile stress was applied in the predefined field to represent the post-tensioning force. The displacement-control loading was applied up to failure.

The concrete's non-linearity was applied through the concrete damaged plasticity (CDP) model. The stress-strain relationship in compression was modeled according to Aslani and Jowkarmeimandi [42], considering a concrete's compressive strength of 35.5 MPa. The concrete behavior in tension was modeled according to Wahalathantri et al. [43]. The constitutive model of CDP for compressive and tensile behavior is shown in **Fig. 7**, and the compressive and tensile concrete parameters are presented in **Table 2a** and **Table 2b**, respectively. The finite element (FE) model developed in ABAQUS® is illustrated in **Fig. 8**.

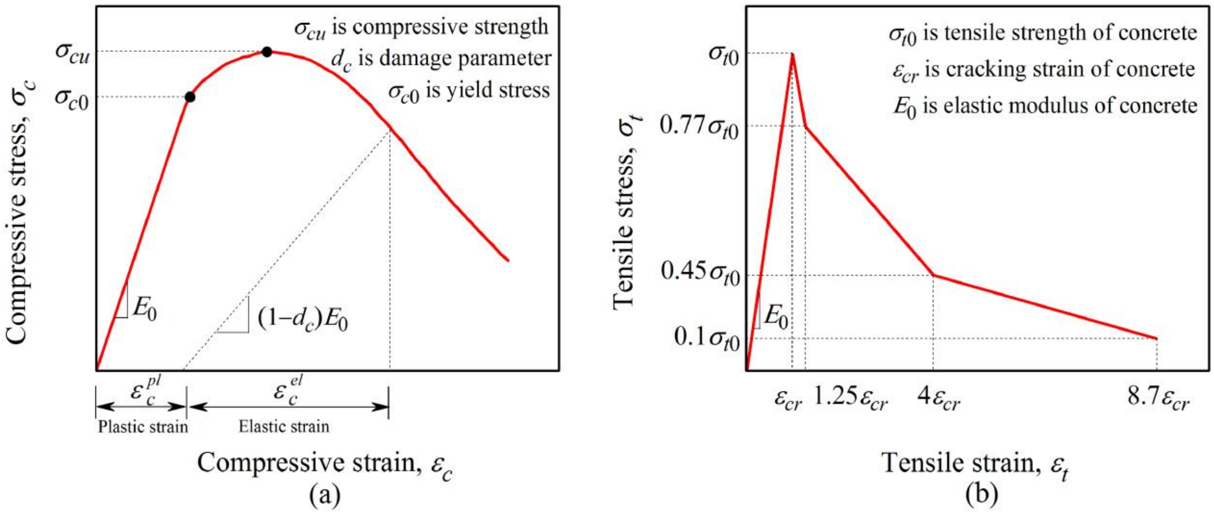

Fig. 7. (a) Compressive behavior and (b) tensile behavior of concrete in the CDP model.

The FE model was validated against experimental findings of a beam set of 35.5 MPa concrete compressive strength and two 12 mm-diameter steel rebars without post-tensioning. The validation, illustrated in **Fig. 9a**, shows that the FEA curve compares well with the experimental results obtained from the average response of three tested beams considering the flexural capacity, with a maximum difference of 1.3%. The deviation between the two approaches is more observed in the initial stage, then decreases in the post-yielding stage, where the results of both approaches are comparable. The deviation in the early behavior can be attributed to the fact that experimental samples of beams are more likely to have defects and minor cracks due to handling while moving and lifting, which can reduce the initial stiffness of the beam. The finite element analysis does not highlight this reduction. However, the flexural capacity is the focus of the current study, which aims to assess the post-tensioning influence of using jute ropes on the flexural capacity of the beam. Hence, the finite element model is deemed valid for further investigation.

4 Results and Discussions

The FE model, validated previously, has been used to evaluate the effectiveness of post-tensioning using jute ropes on flexural capacity. The flexural strength of the non-post-tensioned (control) beam was obtained as 65.5 kN, whereas the post-tensioned beam exhibited 67.8 kN, with a 3.5% improvement. The numerical analysis was extended to include the post-tensioning using four jute ropes.

Table 2a. Compressive parameters for the concrete damaged plasticity (CDP) model

Yield stress	Inelastic strain	d_c
12.93801	0.00000	0.00000
20.74527	0.00031	0.00000
27.28885	0.00062	0.00000
32.01134	0.00094	0.00000
34.69261	0.00125	0.00000
35.50000	0.00156	0.00000
34.39614	0.00187	0.03109
31.57920	0.00218	0.11045
27.88330	0.00249	0.21455
24.00634	0.00281	0.32377
20.37688	0.00312	0.42600
17.18785	0.00343	0.51584
14.48320	0.00374	0.59202
12.23193	0.00405	0.65544
10.37413	0.00436	0.70777
8.84482	0.00468	0.75085
7.58433	0.00499	0.78636
6.54180	0.00530	0.81572
5.67545	0.00561	0.84013
4.95162	0.00592	0.86052
4.34340	0.00623	0.87765
3.82937	0.00655	0.89213
3.39246	0.00686	0.90444
3.01904	0.00717	0.91496
2.69818	0.00748	0.92399
2.42108	0.00779	0.93180

Yield stress is in MPa and d_c is the damage parameter of concrete in compression

Table 2b. Tensile parameters for the concrete damaged plasticity (CDP) model

Yield stress	Cracking strain	d_t
1.96620	0	0
1.09082	7.00×10^{-5}	0.44522
0.77281	0.00015	0.60695
0.60517	0.00022	0.69221
0.50061	0.00029	0.74539
0.42875	0.00037	0.78194
0.37609	0.00044	0.80872
0.33574	0.00052	0.82924
0.30375	0.00059	0.84551
0.27773	0.00066	0.85875
0.25612	0.00074	0.86974
0.23786	0.00081	0.87902
0.22222	0.00088	0.88698
0.20865	0.00096	0.89388
0.19677	0.00103	0.89993
0.18626	0.00111	0.90527
0.17691	0.00118	0.91003
0.16852	0.00125	0.91429
0.16095	0.00133	0.91814
0.15408	0.00140	0.92163

Yield stress is in MPa and d_t is the damage parameter of concrete in tension

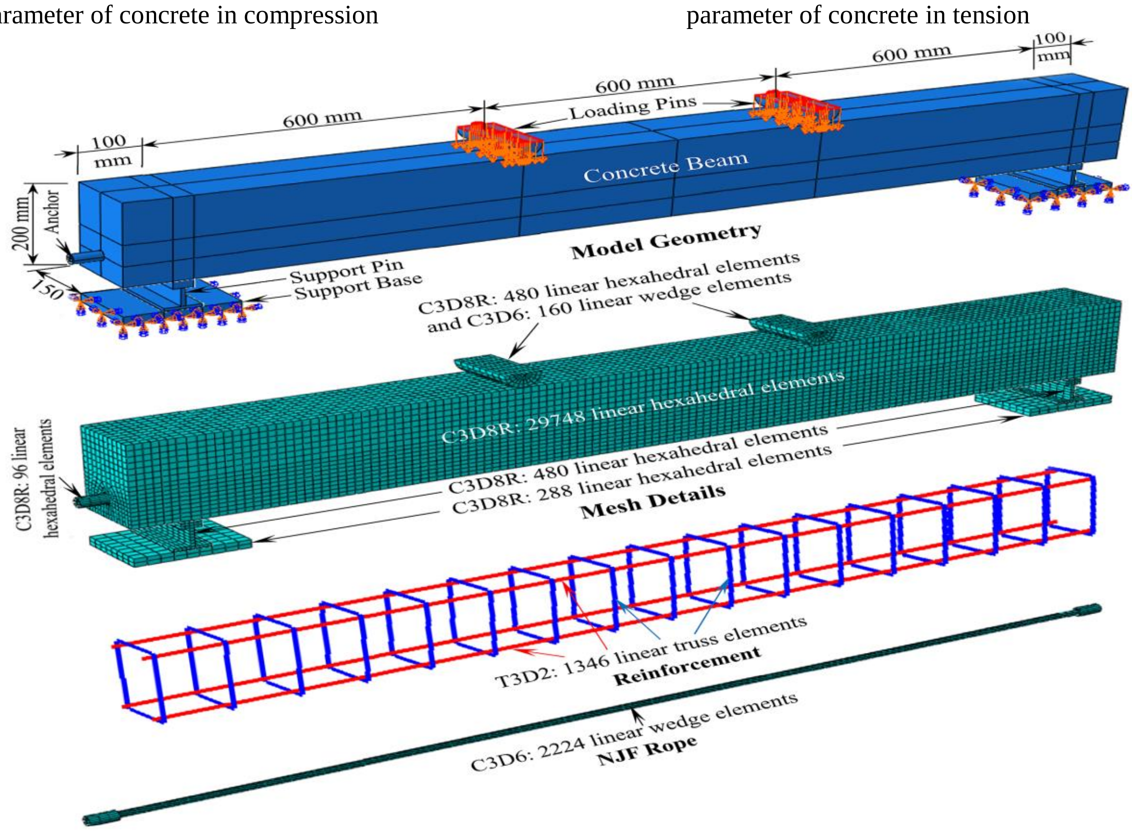

Fig. 8. Finite element (FE) model in ABAQUS®.

Fig. 9b compares the post-tensioned beams at 80% to the control beam. It can be seen that the jute-post-tensioned beam has yielded a 76.2 kN flexural strength compared to 65.5 kN of the control beam (mentioned previously), with a 16.3% premium. **Fig. 9b** also shows two different trends before and after the steel's yielding. Both the control and the post-tensioned beams behave identically in the pre-yielding stage, whereas they start behaving differently in the post-yielding stage. The reason for this phenomenon is the significantly low elastic modulus of the jute ropes, according to strain compatibility, which activated rope contribution upon yielding steel when the deformation rapidly increased.

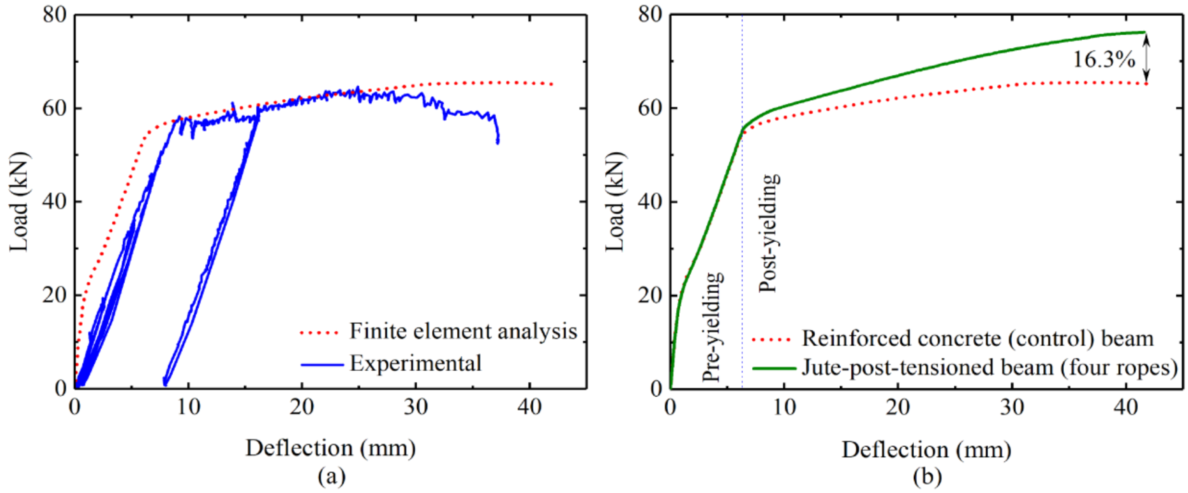

Fig. 9. (a) Validation of the finite element model and (b) Comparison of load–deflection responses of the control and post-tensioned beams.

The effectiveness of beam post-tensioning using jute ropes was compared to steel-post-tensioned beams. The steel strand featured a yield stress of 1466 MPa, a tensile strength of 1723 MPa, and an elastic modulus of 195 GPa [44]. This strand had a 12.7 mm diameter, yielding a cross-sectional area of 92.9 mm ^{2}[45] and allowing it to fit within the duct. It was post-tensioned to 30% of its yield strength. This reduced 30% post-tensioning ratio, compared to 80% for jute ropes, is attributed to the normal concrete strength and the small-scale cross-section investigated in this research. This approach aims to reduce the jacking stress, given that high-strength steel strands are generally employed alongside high-strength concrete and larger-scale elements.

To further capitalize on the benefits of NJF ropes, steel reinforcements were substituted with basalt FRP (BFRP) rebars, thereby completely removing steel and introducing a corrosion-resistant element. The beam analyzed here was reinforced with 8 mm-diameter BFRP rebars with a tensile strength of 966.7 MPa and a 48.7 GPa elastic modulus. Typically, beams reinforced with BFRP rebars should be designed as over-reinforced sections for enhanced ductility, as FRPs are brittle materials, and designing the members for FRP rupture results in a catastrophic failure [46]. However, designing the beam as an over-reinforced section results in a higher flexural capacity than the other beams. Therefore, for comparison, the under-reinforced design was considered with 8 mm diameter BFRP rebars.

Fig. 10 presents a comparison of the flexural behavior across different scenarios: a non-post-tensioned (control) beam reinforced with steel, a beam reinforced with steel and post-tensioned with jute rope, a beam reinforced with steel and post-tensioned with steel, a non-post-tensioned beam reinforced with BFRP rebars, and a beam reinforced with BFRP rebars and post-tensioned with jute ropes. **Fig. 10** shows that the steel strand-post-tensioned beam demonstrated superior flexural performance compared to the others. This case's significant increase in flexural capacity can be attributed to the high-strength steel strands having significantly higher tensile strength than the jute ropes. Nevertheless, the corrosion-resistant properties of jute ropes may offset their comparatively lower strength, thereby promoting their preference over steel strands. Additionally, the beam post-tensioned with jute ropes and reinforced with BFRP rebars achieved a comparable high flexural capacity of 71.6 kN. However, it exhibited significant deflection, similar to all other FRP composites. Considering the service load as the load capacity of the control beam divided by an average load factor of 1.5, resulting in 43.7 kN, it is evident from **Fig. 10** that the post-tensioned beam with jute ropes and reinforced with BFRP rebars has exhibited 26 mm deflection at service load as compared to approximately 5 mm for the other three cases. For a beam span of 1.8 m, the 26 mm deflection exceeds the permissible limit of L/240 (7.5 mm). Compared to steel, the lower stiffness of BFRP results in significant beam deflection upon cracking. This characteristic shifts the design focus from strength to serviceability. Nevertheless, an investigation was carried out to examine the change in structural behavior when post-tensioning the BFRP-reinforced beam with jute ropes as compared to the BFRP-reinforced beam without jute ropes. **Fig. 10** shows that post-tensioning a BFRP-reinforced beam with jute ropes has improved the flexural strength by 18.7% relative to the BFRP-reinforced beam without post-tensioning, which is comparable with the 16.3% improvement observed previously for the steel-reinforced beam post-tensioned with jute ropes. Additionally, the post-tensioning here has reduced the deflection at the service load by 20%, but it still exceeds the permissible limits of 7.5 mm. A matter of interest is that the post-tensioning technique applied to BFRP-reinforced beams has considerably reduced the deflection under service loads, a benefit not observed in steel-reinforced beams. This phenomenon can be justified as the service load for BFRP-reinforced beams exceeds the cracking threshold, leading to a considerable divergence between the load-deflection responses of the control and post-tensioned beams due to significant deformation after cracking. This large deformation activates the jute rope more effectively, enhancing its role in deformation control. Conversely, in steel-reinforced beams, the curves only begin to diverge significantly after yielding; however, the design does not allow service loads to reach this yielding point, which indicates structural failure. As a result, service loads in steel-reinforced beams remain below the yielding threshold, leading to closely aligned curves and clarifying the lack of influence from jute post-tensioning on deflection at service loads in these beams. As previously mentioned, the most superior structural behavior, represented by the highest flexural capacity with the lowest deflection, was observed in the beam reinforced with steel rebars and post-tensioned with steel strands. However, due to the corrosion susceptibility of this beam type, the post-tensioned beam with natural jute fiber ropes and reinforced with steel emerges as the most promising combination.

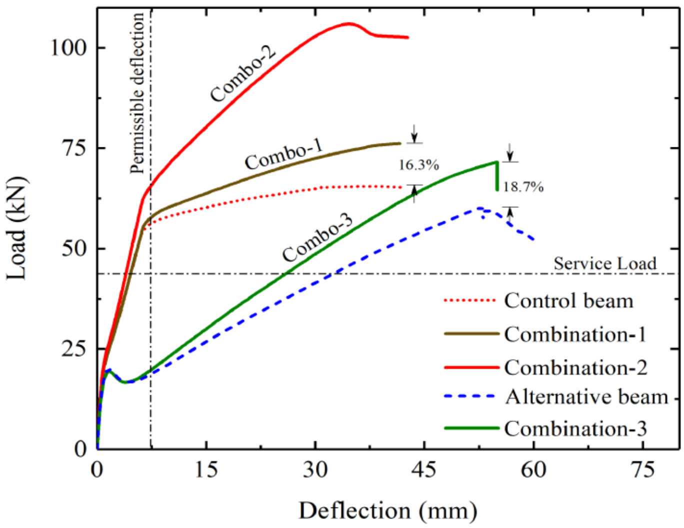

Fig. 10. Comparison of different combinations of post-tensioning and reinforcing materials: Control beam is reinforced with steel; Combination-1 is a beam reinforced with steel and post-tensioned with jute ropes; Combination-2 is a beam post-tensioned and reinforced with steel; Alternative beam is reinforced with BFRP rebars; and Combination-3 is a beam reinforced with BFRP and post-tensioned with jute ropes.

5 Conclusions

The current study explored the potential and effectiveness of natural jute fiber (NJF) ropes for post-tensioning application on structural concrete members. The main conclusions drawn from this research are:

1. Preliminary flexural analysis of beams indicates an increase of 5.9% in flexural strength when post-tensioning with a single NJF rope. Such enhancement appears to increase by up to 23% when the number of NJF ropes is increased to four.

2. The experimental findings on beams post-tensioned using a single NJF rope reveal a 4.3% increase in flexural capacity when compared to beams that are not post-tensioned. This empirical data substantiates the viability of employing natural fiber ropes for post-tensioning applications, indicating improved flexural performance, particularly in increased flexural capacity.
3. Extended investigations using numerical methods reveal improvements of 16.3% in flexural capacity for post-tensioned beams with four ropes from NJF.
4. The beams post-tensioned with steel strands yield the highest flexural capacity, but they pose corrosion risks, which have long been a concern in post-tensioned systems.
5. Replacing steel reinforcement with BFRP bars in the jute-post-tensioned system exhibits a similar trend from a strength perspective, yielding an 18.7% increase in flexural capacity. However, this combination does not meet serviceability criteria, though it reduces the deflection at service load by 20% compared to a non-post-tensioned BFRP-reinforced beam, but it is still above the permissible limit. This limitation is due to the low elastic moduli of both materials.

6 Future Scope

The proposed technique has demonstrated efficacy in improving structural behavior while concurrently facilitating the flexible replacement of the unbonded ropes as needed. However, it should be noted that the ropes' exposure to weather and chemical agents accelerates their degradation, alongside the need for continuous monitoring and maintenance of anchorage. This presents opportunities for future research into the application of bonded natural fiber ropes in post-tensioning and/or pretensioning systems. Additionally, while this study primarily addresses post-tensioning in beams, the methodology may also be applied to secondary structural elements within buildings.

Funding Statement

This work has been supported by the Italian Ministry of University and Research (MUR) - PRIN PROJECT titled 'Automated Reinforcement Manufacturing for COncrete COnstruction Decarbonisation - ARMCO$_2$D' (PROJECT CODE: P2022YK392, CUP: D53D23018590001), and ASEM-DUO-India Professor Fellowship Award.

CRediT authorship contribution statement

Ali Alraie: Writing – review & editing, Writing – original draft, Visualization, Investigation, Data curation, and Conceptualization. **Saverio Spadea**: Writing – review & editing, Supervision, and Conceptualization. **Vasant Matsagar**: Writing – review & editing, Supervision, and Conceptualization.

Conflicts of Interest

The authors declare that they have no known competing financial interests or personal relationships that could have appeared to influence the work reported in this paper.

Data Availability Statement

All data that support the findings of this study are available from the corresponding author upon reasonable request.

References

[1] Thiruchitrambalam M, Athijayamani A, Sathiyamurthy S, Thaheer ASA. A review on the natural fiber-reinforced polymer composites for the development of roselle fiber-reinforced polyester composite. Journal of Natural Fibers 2010; 7(4): 307–323. https://doi.org/10.1080/15440478.2010.529299.

[2] Mohanty AK, Misra M, Drzal LT (Eds.). Natural fibers, biopolymers, and biocomposites (1st ed.). CRC Press 2005. https://doi.org/10.1201/9780203508206.

[3] Abedi M, Hassanshahi O, Rashiddel A, Ashtari H, Meddah MS, Dias D, Choong KK. A sustainable cementitious composite reinforced with natural fibers: An experimental and numerical study. Construction and Building Materials 2023; 378: 131093. https://doi.org/10.1016/j.conbuildmat.2023.131093.

[4] Liu K, Jayaramana D, Shib Y. Bamboo: A very sustainable construction material & the 3rd world symposium on sustainable Bio-composite materials and structures. In the 2022 International Conference summary report. Sustainable Structures 2023; 3(2): 000033. 10.54113/j.sust.2023.000033.
[5] Singh AK, Mukesh K, Mitra S. Carbon footprint and energy use in jute and allied fibre production. The Indian Journal of Agriculture Science 2018; 88(8): 1305–1311. https://doi.org/10.56093/ijas.v88i8.82579.
[6] Navaratnam S, Selvaranjan K, Jayasooriya D, Rajeev P, Sanjayan J. Applications of natural and synthetic fiber reinforced polymer in infrastructure: A suitability assessment. Journal of Building Engineering 2023; 66: 105835. https://doi.org/10.1016/j.jobe.2023.105835.
[7] Saini K, Matsagar VA, Kodur VR. Recent advances in the use of natural fibers in civil engineering structures. Construction and Building Materials 2024; 411: 134364. https://doi.org/10.1016/j.conbuildmat.2023.134364.
[8] Ali M. Use of coconut fibre reinforced concrete and coconut-fibre ropes for seismic-resistant construction. Materiales de Construccion 2016; 66(321): e073. https://doi.org/10.3989/mc.2016.01015.
[9] Ramakrishna G, Sundararajan T. Studies on the durability of natural fibres and the effect of corroded fibres on the strength of mortar. Cement and Concrete Composites 2005; 27(5): 575-582. https://doi.org/10.1016/j.cemconcomp.2004.09.008.
[10] Wang X, Petrů M, Yu H. The effect of surface treatment on the creep behavior of flax fiber reinforced composites under hygrothermal aging conditions. Construction and Building Materials 2019; 208: 220-227. https://doi.org/10.1016/j.conbuildmat.2019.03.001.
[11] Ramaswamy HS, Ahuja BM, Krishnamoorthy S. Behaviour of concrete reinforced with jute, coir and bamboo fibres. International Journal of Cement Composites and Lightweight Concrete 1983; 5(1): 3–13. https://doi.org/10.1016/0262-5075(83)90044-1.
[12] Daba ET, Zelleke DH, Matsagar VA, Bishnoi S, Kodur VR. Characterization of plant-based natural fiber ropes for potential futuristic application as reinforcement in concrete structures. Journal of Natural Fibers 2024; 21(1): 2397703. https://doi.org/10.1080/15440478.2024.2397703.
[13] Cook DJ, Pama RP, Weerasingle HLSD. Coir fibre reinforced cement as a low cost roofing material. Building and Environment 1978; 13(3): 193–198. https://doi.org/10.1016/0360-1323(78)90043-4.
[14] Reis JML. Fracture and flexural characterisation of natural fiber-reinforced polymer concrete. Construction and building materials 2006; 20(9): 673–678. https://doi.org/10.1016/j.conbuildmat.2005.02.008.
[15] Pacheco-Torgal F, Jalali S. Cementitious building materials reinforced with vegetable fibres: A review. Construction and building materials 2011; 25(2): 575–581. https://doi.org/10.1016/j.conbuildmat.2010.07.024.
[16] Chen CLH, Dauletbek A, She, F, Hui D, Gaff M, ... Ashraf M. Properties and applications of bamboo fiber-A current-state-of-the art. Journal of Renewable Materials 2021; 10(3): 605–624. https://doi.org/10.32604/jrm.2022.018685.
[17] Sathiparan N, Subramaniam DN. Optimizing fly ash and rice husk ash as cement replacements on the mechanical characteristics of pervious concrete. Sustainable Structures 2025; 5(1): 000065. 10.54113/j.sust.2025.000065.
[18] Gómez PJ, Yero AM, Riverón GC. Design and construction of houses with Guadua cane and rice husk in Ecuador as an alternative to local development. Sustainable Structures 2024; 4(2): 000047. 10.54113/j.su st.2024.000047.
[19] Zhou X, Ghaffar SH, Dong W, Oladiran O, Fan M. Fracture and impact properties of short discrete jute fibre-reinforced cementitious composites. Materials & Design 2013; 49: 35–47. https://doi.org/10.1016/j.matdes.2013.01.029.
[20] Acosta-Calderon S, Gordillo-Silva P, García-Troncoso N, Bompa DV, Flores-Rada J. Comparative evaluation of sisal and polypropylene fiber reinforced concrete properties. Fibers 2022; 10(4): 31. https://doi.org/10.3390/fib10040031.
[21] Abdel Hafez RD, Shubbar A, Nasr MS, Ftahd AA. Reinforcing the brittle resistance of high strength concrete using agricultural waste fiber. Sustainable Structures 2024; 4(3): 000058. https://doi.org/10.54113/j.sust.2024.000058.
[22] Di Sarno L, Albuhairi D, Medeiros JMP. Exploring innovative resilient and sustainable bio-materials for structural applications: Hemp-fibre concrete. Structures 2024; 68: 107096. https://doi.org/10.1016/j.istruc.2024.107096.
[23] Ren G, Yao B, Ren M, Gao X. Utilisation of natural sisal fibers to manufacture eco-friendly ultra-high performance concrete with low autogenous shrinkage. Journal of Cleaner Production 2022; 332: 130105. https://doi.org/10.1016/j.jclepro.2021.130105.
[24] Heniegal AM. Performance of concrete beams reinforced with fiber ropes as a partial replacement of steel bars. International Journal of Engineering and Innovative Technology 2017; 7(3): 25–33. 10.17605/OS F.IO/6UQSY.
[25] Varma DA, Sarker PK, Madhavan MK, Jayanarayanan K. Experimental and analytical assessment of strengthening of concrete cylinders using jute/basalt hybrid textile fiber reinforced mortar. Structures 2024;

70: 107807. https://doi.org/10.1016/j.istruc.2024.107807.
[26] Alam MA, Nouri K, Jumaat MZ, Muda ZC. Flexural strengthening of reinforced concrete beam using jute rope composite plate. In The Third National Graduate Conference 2015; 8–9.
[27] Huang L, Yan B, Yan L, Xu Q, Tan H, Kasal B. Reinforced concrete beams strengthened with externally bonded natural flax FRP plates. Composites Part B: Engineering 2016; 91: 569–578. https://doi.org/10.1016/j.compositesb.2016.02.014.
[28] Limwibul V, Jirawattanasomkul T, Jongvivatsakul P, Likitlersuang S, Dai JG, Ueda T. Stress-strain behaviour of pre-damaged concrete confined with natural fibre reinforced polymer. Structures 2024; 69: 107434. https://doi.org/10.1016/j.istruc.2024.107434.
[29] Yooprasertchai E, Wiwatrojanagul P, Pimanmas A. A use of natural sisal and jute fiber composites for seismic retrofitting of nonductile rectangular reinforced concrete columns. Journal of Building Engineering 2022; 52: 104521. https://doi.org/10.1016/j.jobe.2022.104521.
[30] Bitar R, Saad G, Awwad E, El Khatib H, Mabsout M. Strengthening unreinforced masonry walls using natural hemp fibers. Journal of Building Engineering 2020; 30: 101253. https://doi.org/10.1016/j.jobe.2020.101253.
[31] Abdulla KF, Cunningham LS, Gillie M. Out-of-plane strengthening of adobe masonry using hemp fibre ropes: An experimental investigation. Engineering Structures 2021; 245: 112931. https://doi.org/10.1016/j.engstruct.2021.112931.
[32] Trochoutsou N, Di Benedetti M, Pilakoutas K, Guadagnini M. Tensile performance of lime-based natural-fibre composites as strengthening systems for masonry. Academic Journal of Civil Engineering 2019; 37(2): 314–320. https://doi.org/10.26168/icbbm2019.45.
[33] Mercedes L, Bernat-Maso E, Gil L. Numerical simulation of masonry walls strengthened with vegetal fabric reinforced cementitious matrix (FRCM) composites and subjected to cyclic loads. Structures 2022; 35: 1232–1242. https://doi.org/10.1016/j.istruc.2021.09.010.
[34] Saini K, Spadea S, Matsagar VA. Flexural behavior of natural fiber-reinforced foamed concrete beams. Architecture, Structures and Construction 2024; 4(2): 157–172. https://doi.org/10.1007/s44150-024-00114-2.
[35] Alraie A, Spadea S, Matsagar V. Enhanced sustainability through strengthening of existing structures with natural fibre ropes. Procedia Structural Integrity 2024; 64: 1943–1950. https://doi.org/10.1016/j.prostr.2024.09.266.
[36] Sanal I, Verma D. Construction materials reinforced with natural products. In: Martínez, L, Kharissova, O, Kharisov, B (eds) Handbook of Ecomaterials. Springer, Cham 2018. https://doi.org/10.1007/978-3-319-48281-1_75-1.
[37] Darwin D, Dolan CW, Nilson AH. Design of concrete structures. McGraw-Hill Education 2016. New York (NY), USA.
[38] American Concrete Institute (ACI) Committee 440. Prestressing concrete structures with FRP tendons. ACI 440.4R-04. American Concrete Institute (ACI) 2004. Farmington Hills, MI, USA. https://doi.org/10.1061/40753(171)160.
[39] Grace NF, Singh SB. Design approach for carbon fiber-reinforced polymer prestressed concrete bridge beams. ACI Structural Journal 2003; 100(3): 365–376. 10.14359/12612.
[40] Tahir M, Karam MS, Hassam M, Umer M, Hameed R. Numerical evaluation of axial compressive behavior of hollow concrete columns reinforced with GFRP bars and spirals. Structural Concrete 2024; 25: 566-582. https://doi.org/10.1002/suco.202201045.
[41] Tahir M, Wang Z, Wei Z, Jameel R. Numerical and analytical modeling of FRP-reinforced concrete columns subjected to compression loading. Australian Journal of Structural Engineering 2021; 22(2): 96-109. https://doi.org/10.1080/13287982.2021.1923158.
[42] Aslani F, Jowkarmeimandi R. Stress–strain model for concrete under cyclic loading. Magazine of Concrete Research 2012; 64(8): 673–685. https://doi.org/10.1680/macr.11.00120.
[43] Wahalathantri B, Thambiratnam D, Chan T, Fawzia S. A material model for flexural crack simulation in reinforced concrete elements using ABAQUS. In Proceedings of the First International Conference on Engineering, Designing and Developing the Built Environment for Sustainable Wellbeing 2011; 260–264. Queensland University of Technology.
[44] Raju NK. Prestressed concrete. Tata McGraw Hill 2012, New Delhi, India.
[45] American Society for Testing and Materials (ASTM) Committee A01. Standard specification for steel strand, uncoated seven-wire for prestressed concrete. A416/A416M-06. ASTM International 2006, West Conshohocken, USA. 10.1520/A0416_A0416M-06.
[46] Yang Y, Orr J, Spadea S. Shear behavior of variable-depth concrete beams with wound fiber-reinforced polymer shear reinforcement. Journal of Composites for Construction 2018; 22(6): 04018058. 10.1061/(ASCE)CC.1943-5614.0000899